# Impact of the structural properties of holmium doped ZnO thin films grown by sol–gel method on their optical properties

M Popa, L.C. Pop, Guy Schmerber, Corinne Bouillet, Ovidiu Ersen

# Impact of the structural properties of holmium doped ZnO thin films grown by sol-gel method on their optical properties

M. Popa[1,2], L.C. Pop[1], G. Schmerber[2], C. Bouillet[2], O. Ersen[2]

[1] *Faculty of Chemistry and Chemical Engineering, Babes-Bolyai University, Arany János 11, 400028 Cluj-Napoca, Romania*

[2] *Institut de Physique et Chimie des Matériaux de Strasbourg (IPCMS), UMR 7504 CNRS - Université de Strasbourg, 23 rue du Loess, BP 43, 67034 Strasbourg Cedex 2, France*

**Keywords:** Ho doped ZnO, thin films, Photoluminescence

## Abstract

Polycrystalline Ho (1, 3, 5 at %) doped ZnO thin films were prepared by sol-gel method. The films show a pure wurtzite crystalline structure. The particle size decreases from 29 to 9 nm when the Ho concentration increases from 0 to 5 at %. They present a homogeneous morphology for the specimens containing 1 and 3 at % of Ho. At 5 at % Ho the morphology of the film changes and the particles agglomerate in larger clusters. The UV-Vis transmission was found higher than 70% and a decreasing of the band gap from 3.28 to 3.22 eV was observed with the increase of the Ho concentration. The $^5F_5 \rightarrow ^5I_8$ Ho transition at ~ 662 nm can be easily identified in the photoluminescence (PL) spectra, using an UV excitation source. A combined analysis of the photoluminescence properties at the room temperature and of the morphological and structural characteristics of the films allows us to directly link the Ho emission to the Ho incorporation in ZnO matrix.

## 1. Introduction

In the recent years, ZnO alongside with $TiO_2$[1, 2] have become one of the most popular and promising material for many applications like spintronic or optoelectronic devices, solar cells, transparent conductors, sensors, photocatalysis. ZnO is a wide band gap (3.37 eV), naturally n-type semiconductor, which is also biocompatible, biodegradable and nontoxic.[3] It is generally admitted that this inorganic compound is one of the most interesting materials thanks to the possibility to easily tune its properties by changing the synthesis methods, the chemical environment, the doping etc. according to some specific requirements in industrial applications. In this context, doping with transition metals or non-metals was also regularly employed in order to modify the properties of pure ZnO.[4] Rare earths (RE) doped ZnO was also subject of many papers during the last years.[5-24] One of the main interest in using trivalent rare earths doping lies in the possibility to use them as optical activators. They can generate narrow and intense emission lines due to their 4*f* intrashell transitions. RE doped ZnO thin films attract considerable attention because of their possible application in solar cells, when it is possible to increase the conversion efficiency up to 35 – 40% by adding a down-conversion wide band gap semiconducting oxide doped with RE ions at the top of a silicon-based conventional solar cell.[25] The down-conversion process consists in transforming incident high-energy photons into two or more photons of smaller energy. Regarding the ZnO-based materials, the main obstacle in achieving this goal is the lack or poor luminescent response of the RE doped ZnO, especially when red light emissions are desired. In order to overcome this inconvenient, several attempts were performed, for example extrinsic defects addition by using $Li^+$ [26] or chlorine[27] impurities. In more recent works, the presence of intrinsic defects such as oxygen vacancies was considered responsible for mediating the energy transfer between the ZnO host and RE.[28] Nevertheless, a clear understanding of the energy transfer process is not yet achieved.

Trivalent holmium is an additional lanthanide ion which possesses energy levels in the red and NIR ($^5F_5$ and $^5I_4$) region of the spectrum along with a relatively long live of the energy level ($^5I_7$). Holmium was successfully used for upconversion, when a low energy radiation (e.g., near infrared radiation) is transformed in emission at shorter wavelengths (visible or near UV).[29] Bulk and single crystal holmium doped ZnO was subject to intense research during the last years.[18, 19, 23, 30-34] Only few studies were dedicated to Ho doped ZnO thin films,[16, 32] and even fewer on Ho doped ZnO thin films grown by sol-gel method[35]. This method is a well-known, industrially scale spread process and particularly adapted to produce films in a simple, low-cost and highly-controlled way. Furthermore, it generally leads to

polycrystalline ZnO which may be considered more interesting than single-crystal ZnO since RE luminescence centers could be localized at the ZnO grain boundaries.[16] According to our knowledge, no visible emissions were observed so far for Ho doped ZnO bulk, single-crystal or epitaxial films, using UV light excitation.[16, 23]

In this paper, the relation between the optical properties at room temperature and the structural and morphological properties of Ho doped ZnO thin films was investigated. More precisely, our work reports on the sol-gel synthesis of the Ho doped ZnO thin films and their characterization in order to provide a deeper understanding of the holmium induced properties with respect to the ZnO matrix. With respect to other previous reported results, the expected red light emission of Ho ions will be discussed in relation with the dynamic process of energy transfer in the films, considering that a certain number of Ho ions are incorporated in ZnO matrix. Such a combined structural and optical study requires the use of various characterization techniques such as X-ray diffraction (XRD), UV-Vis spectroscopy, photoluminescence (PL), Hall measurement, scanning electron microscopy (SEM), transmission electron microscopy in conventional bright field TEM and in the STEM-HAADF mode and EELS spectroscopy.

## 2. Experimental conditions

### 2.1. Sample preparation

Sol-gel method and spin-coating process were used for obtaining Ho doped ZnO thin films. Undoped ZnO thin films were prepared following the steps previously presented.[4] For doping, a homogeneous solution was prepared by dissolving zinc acetate dihydrate ZnAc (0.7 м) (Merck, 99.5%) and holmium (III) nitrate pentahydrate (Aldrich, 99,99%) -1, 3, and 5 at % Ho- in absolute ethanol (Sigma Aldrich, 99.5%). Ethanolamine (EA) (Alfa Aesar, 98%) has been added as a complexing agent in order to obtain a clear solution. The quartz substrate was cleaned in ethanol / acetone / ethanol (5 min) and subsequently dried under nitrogen gas flow before deposition. The deposition process of the thin films was performed by spin-coating using 3000 rpm for 30 s. The films were deposited in 3 layers on the substrate and were pre-heated at 300 °C for 5 min, after the deposition of each layer. The final thermal treatment was performed at 500 °C for 2 hours, in air (with heating rate of 20 degrees/min until reaching 500 °C, using a CARBOLITE furnace).

**Sample characterization**

High resolution X-ray diffraction (HRXRD) was employed, using a PB-Ge(220)x2 Rigaku - SmartLab X-ray diffractometer. The particles size was calculated by Scherrer formula, by using the (002) diffraction peak.

The optical properties of the films were studied by using a Perkin-Elmer Lambda 950 spectrophotometer for the absorption and transmission experiments. The band gap was calculated using the formula:

$$\alpha h\upsilon = A(h\upsilon - Eg)^n \quad (1)$$

where $\alpha h\upsilon$ is the absorption coefficient, $A$ is a constant, $h$ is the Planck constant, $\upsilon$ is the frequency, $Eg$ is the semiconductor band gap and $n = 1/2$, considering a direct semiconductor.

Room temperature PL experiments were performed, using 355 nm excitation line, given by a frequency-tripled neodymium-doped yttrium aluminum garnet (Nd-YAG) laser.

The surface morphology has been observed using a JEOL JSM-6700F scanning electron microscope (SEM) coupled with an energy dispersive x-ray spectroscopy (EDX).

The transmission electron microscopy analyses were performed in TEM and scanning TEM (STEM) mode using a JEOL 2100F (imaging filter, EDX, biprism, 2 CCD cameras) microscope operating at 200 kV, equipped with a spherical aberration probe corrector and a GIF Tridiem EELS spectrometer. HAADF imaging was systematically used in STEM; this incoherent mode provides images with a high contrast, principally related to the atomic number of the specimen and to its thickness, facilitating thus the interpretation of the images acquired on complex specimens from a morphological point of view.

## 3. Results and discussion

X-ray diffraction patterns of the Ho doped ZnO thin film samples are presented in Figure 1. The doped and undoped ZnO thin films present a hexagonal crystal symmetry since all the peaks fit with the ZnO wurtzite structure and no indication of the presence of a secondary phase is found. Undoped ZnO diffractogram indicates the presence of two small peaks corresponding to (100) and (101) Miller plans and a sharp peak at $2\theta = 34.40°$. Such a pattern can be unambiguously assigned to a polycrystalline film with a textured structure, oriented along the (002) plan. A considerable decrease of the intensity of the (002) peak can be observed by increasing the Ho concentration. In addition, a small shift of the peak

position ($2\theta = 34.30°$) can be observed for the sample with 5 at % of Ho. The mean grain size, determined from the Scherrer formula, decreases about 3 times when the Ho concentration increases from 0 to 5 at % (Figure 1).

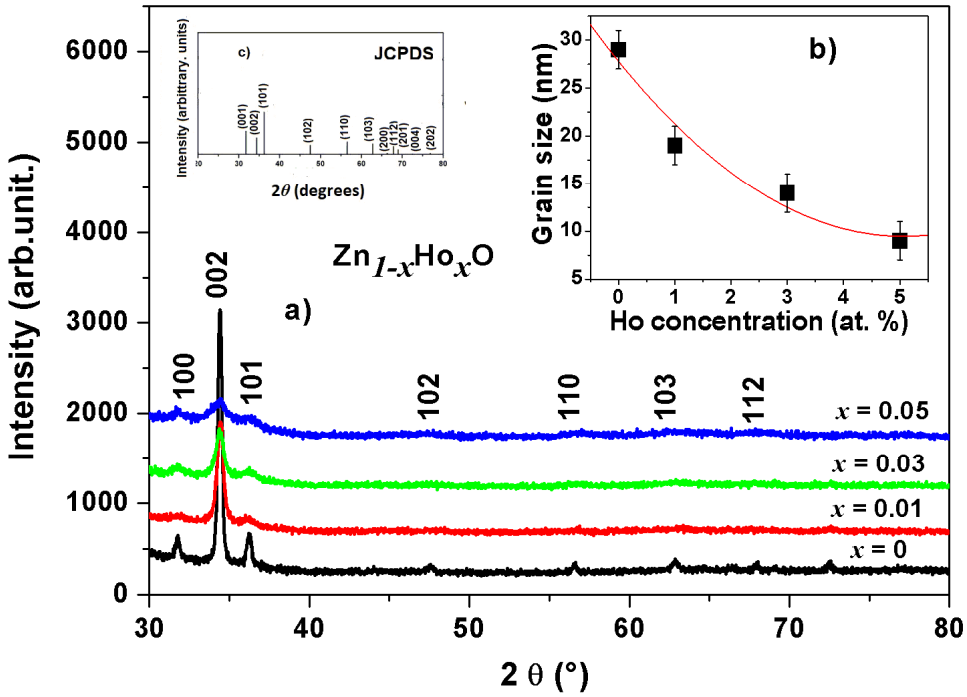


**Figure 1:** a) XRD patterns of $Zn_{1-x}Ho_xO$ ($x$ = 0, 0.01, 0.03, 0.05) thin films, thermally treated at 500 °C, deposited on quartz substrates, b) crystallite size evolution as a function of Ho concentration, c) ZnO wurtzite crystalline structure according JCPDS.

The lattice parameters $a$ and $c$ of the Ho doped ZnO samples are presented in Table 1. The $c$ parameter increases when the Ho concentration change from 3 and 5 at % and is slightly affected by the Ho doping at 1 at % as compared to pure ZnO. The increasing of the $c$ parameter is in general associated to the incorporation of the dopant atoms in the lattice.[36] However, this statement requires additional proofs, in addition to the results obtained from XRD, before a complete validation. At low concentrations of Ho (<1%) the difference is probably not significant with respect to the measurement accuracy however for the higher concentration the difference is totally reliable (see the values for 0.03 and 0.05).

**Table 1:** Lattice parameters (determined from XRD), concentration and thickness (determined from SEM analysis), of the $Zn_{1-x}Ho_xO$ ($x$ = 0, 0.01, 0.03, 0.05) thin films, thermally treated at 500 °C.

| Ho nominal atomic concentration [$x$] | SEM (EDX) analysis | | XRD analysis | | |
|---|---|---|---|---|---|
| | Experimental atomic concentration | Thickness [nm] ± 10 nm | Cell parameters [Å] | | Cell volume [Å$^3$] |
| | | | $a$ | $c$ | |
| 0 | 0 | 250 | 3.251(9) | 5.209(8) | 47.704(4) |
| 0.01 | 0.026 ± 0.003 | 205 | 3.248(6) | 5.206(3) | 47.580(3) |
| 0.03 | 0.04 ± 0.004 | 190 | 3.252(6) | 5.215(0) | 47.779(9) |
| 0.05 | 0.07 ± 0.006 | 240 | 3.252(6) | 5.224(5) | 47.867(0) |

UV-Vis transmission spectra are presented in Figure 2. All the films present a high transmission (over 70%). A diminution of about 20% of the transmission can be observed for the 5 at % Ho doped ZnO film, comparing with the other samples. The same tendency was observed by others authors,[25] when ZnO was doped with 5 at % Yb. The band gap energy of the samples, calculated from the plot of $(\alpha h\nu)^2$ versus $h\nu$, indicates an exponential decreasing from 3.28 to 3.22 eV when the Ho doping increases to 5 at %. (Figure 2). The as-deduced band gap energies are similar with other reported values on Yb doped ZnO.[25]

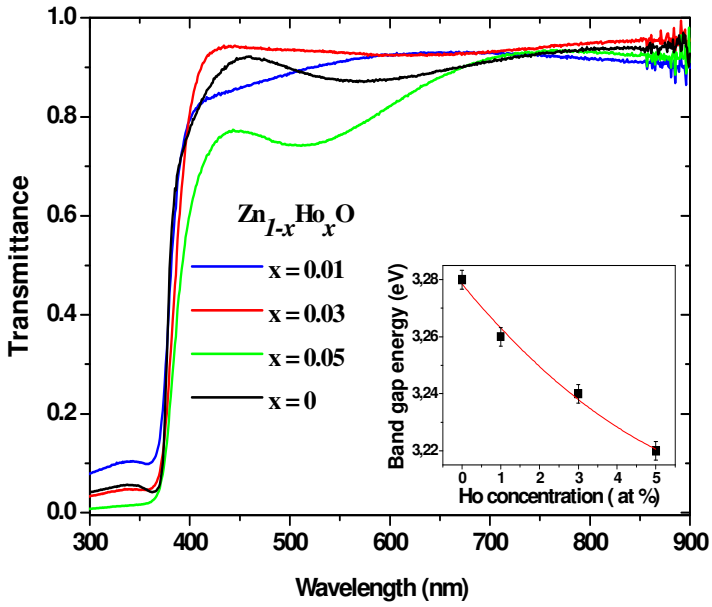

**Figure 2:** Transmission spectra as a function of Ho concentration of the $Zn_{1-x}Ho_xO$ thin films, thermally treated at 500 °C. Inset: the variation of the band gap energy as a function of Ho concentration for the same films.

Figure 3 shows the SEM images of $Zn_{1-x}Ho_xO$ ($x$ = 0, 0.01, 0.03, 0.05) and undoped ZnO thin films. As can be seen, the undoped ZnO and $Zn_{1-x}Ho_xO$ ($x$ = 0.01, 0.03) present a homogenous structure, with the particle size progressively decreasing when the doping amount increases. By contrast, the SEM image of $Zn_{0.95}Ho_{0.05}O$ film presents a non-homogenous morphological structure, with small particles agglomerated in larger clusters. The effective Ho concentrations determined by EDX and the thickness of the films are presented in the Table 1.

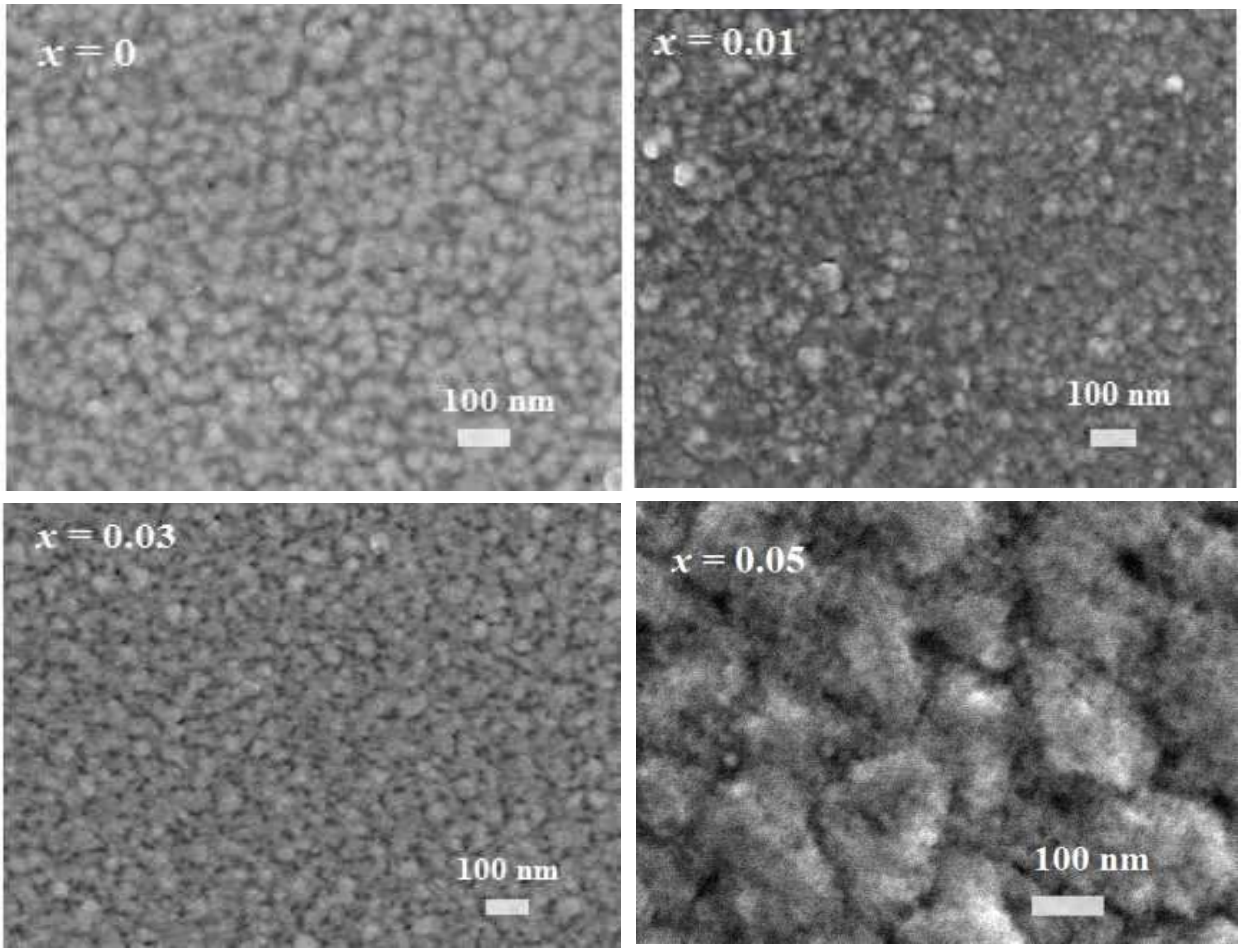

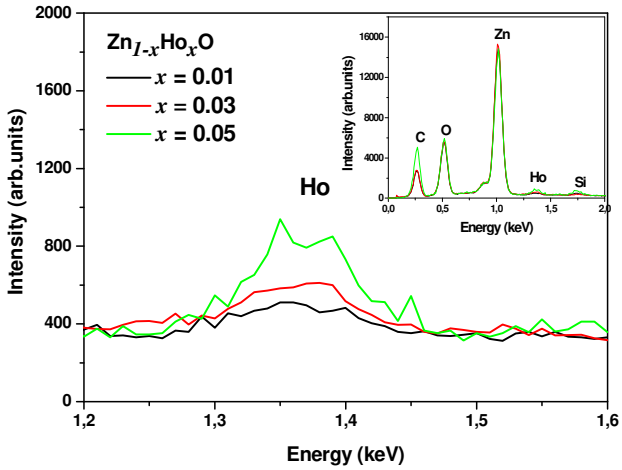


**Figure 3:** SEM images and EDX spectra of $Zn_{1-x}Ho_xO$ ($x$ = 0.01, 0.03, 0.05) thin films, thermally treated at 500 °C.

The cross-section TEM images obtained on Ho doped ZnO samples indicate a porous structure of the films, where the three layers deposited on the substrate are well visible. Moreover, we observed that the surface of each layer is denser than the rest of the film and the density of the corresponding areas increases with the number of thermal treatments (the first layer was three times thermally treated at 500 °C for 5 min). In accord with the XRD results, the HRTEM images and corresponding FFT patterns (Figure 5) indicate a wurtzite crystallographic structure oriented mainly along the [002] crystallographic axis.

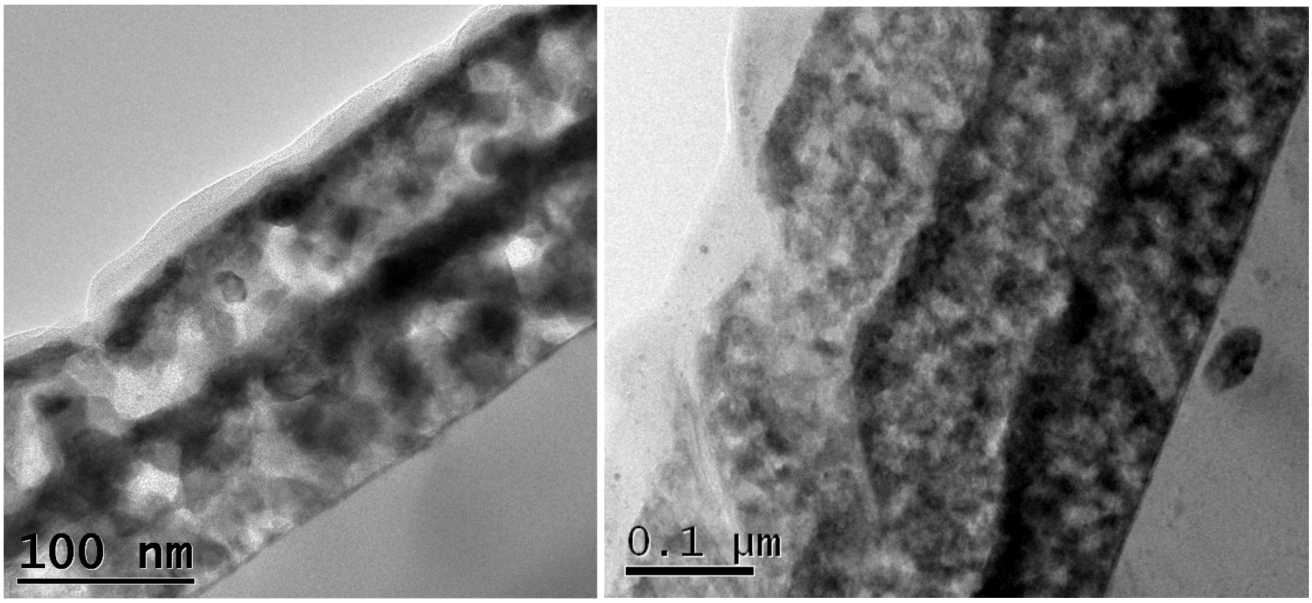


**Figure 4.** Cross-section TEM images of undoped (left) and 1 at% Ho doped (right) thin films.

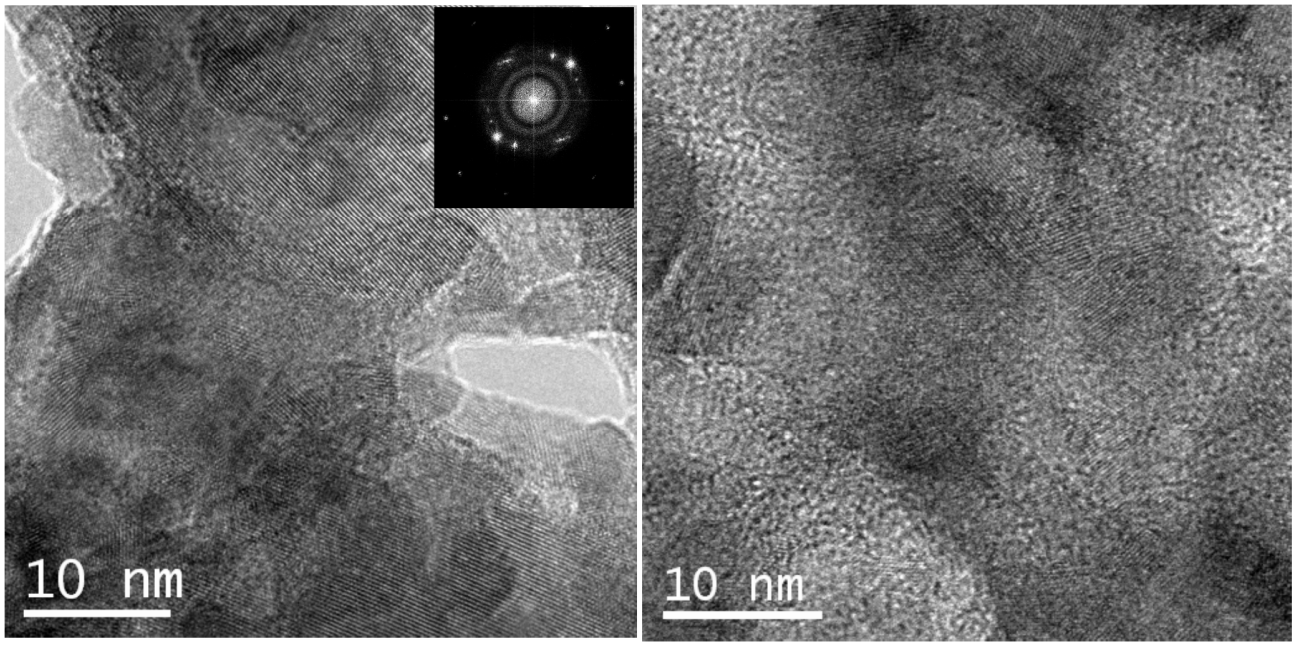


**Figure 5.** HRTEM images and FFT pattern of undoped (left) and 5 % Ho doped ZnO (right).

EELS spectra acquired on 5 at % Ho doped ZnO thin film prepared in cross section confirms the presence of Ho ions in the films (Figure 6). As can be seen in Figure 7, Ho ions are well distributed in the dense but also in the less dense (porous) areas of the film. By contrast, we were not able to detect the presence of Ho ions in the 1 and 3 at % Ho doped ZnO samples, very probably due to the chemical

sensitivity of the EELS technique (few at %). However, the results obtained on the 5 at % thin films suggest that Ho atoms have a homogeneous distribution in the films, without a significant agglomeration of clustering at specific locations at the nanometer level.

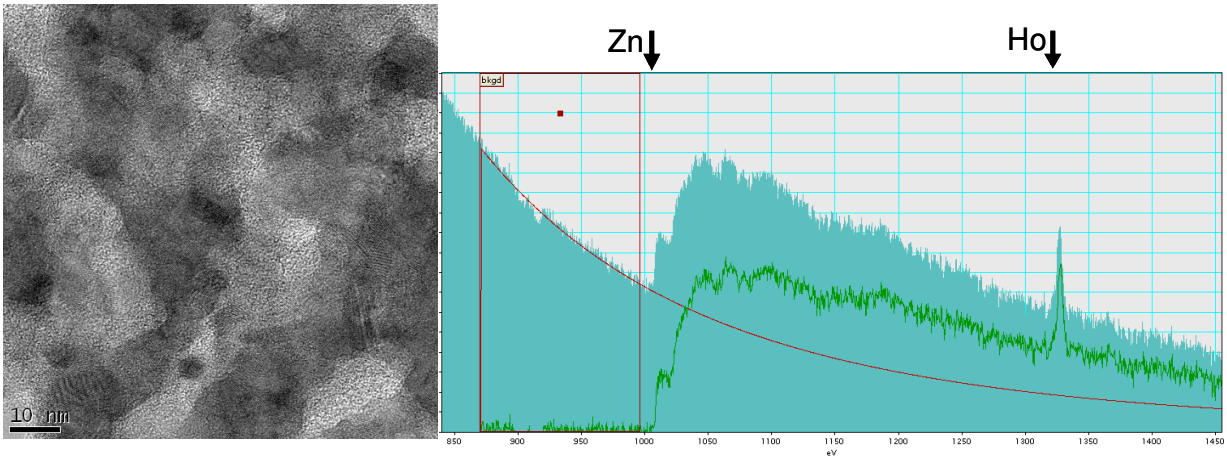


**Figure 6.** TEM image and the corresponding EELS spectrum of the 5 at % Ho doped ZnO sample, which provides direct evidence of the presence of Ho in the film.

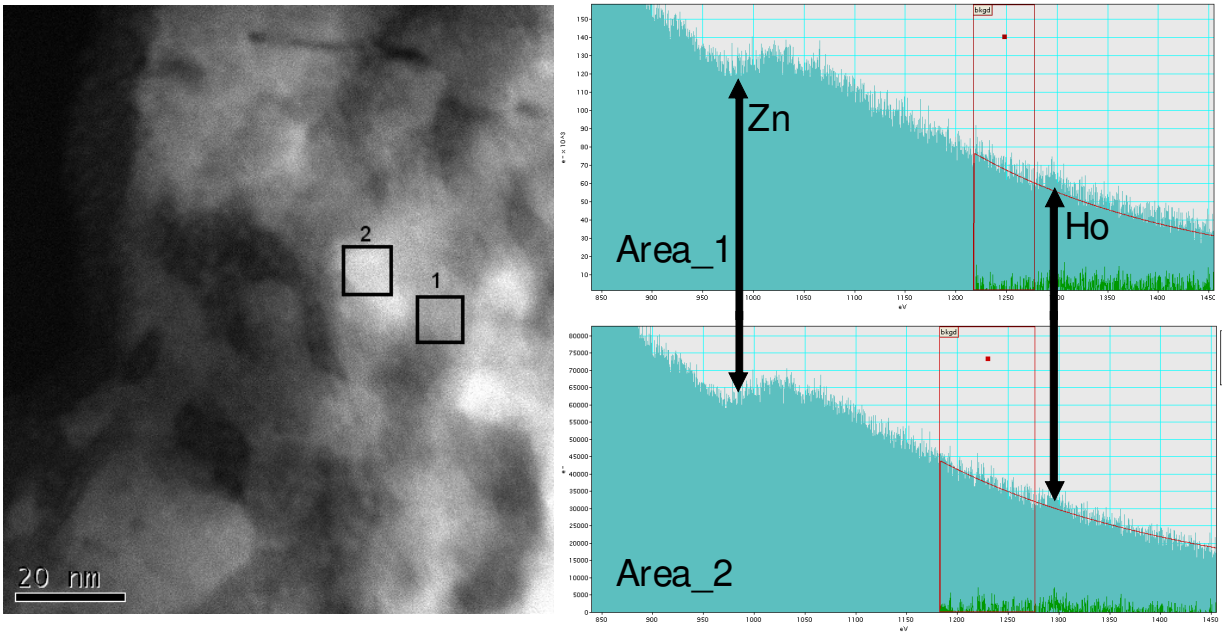


**Figure 7.** STEM-HAADF image of 5 at % Ho doped ZnO thin film and EELS spectra acquired at Ho edge 1) in a porous (less denser) area, showing that Ho ions are present in both areas (their lateral size is about 10 nm), 2) a denser area.

PL measurements at room temperature were performed in order to assess the optical properties of these Ho doped ZnO films prepared by sol-gel method (Figure 8). The samples were excited using a 355 nm laser line. The peaks at 532 and 710 nm in the PL spectra corresponds to the laser line of 1.5 and the double frequency, respectively. In the undoped ZnO thin film (Figure 8 a) and c)), a main peak centered at ~ 385 nm (3.22 eV) can be observed. After Gaussian deconvolution, three bands at about 371 nm (3.34 eV), 385 nm (3.22 eV) and ~ 400 nm (3.1 eV) can be identified. The band at 3.34 eV can be associated with the excitons emission, due to their band edge transition. The dominant band at 3.22 eV could be attributed to the presence of an unidentified donor level situated ~ 0.12 eV below the conduction band (CB) while the band at 3.1 eV could be related to the electron transition from an interstitial zinc ($Zn_i$) level to valence band (VB).[37, 38] In the Ho doped ZnO samples, the peak positions are shifted and centered at ~ 388 nm, for 3 at % and strongly shifted to the visible region of the spectrum (~ 420 nm) for 5 at % Ho (Figure 8 a), d), e), f)). After Gaussian deconvolution, no relevant modification of the bands positions was observed in 1 at % Ho doped ZnO, as compared to the undoped ZnO (Figure 8 c)). Also, the presence of the excitonic emission situated at 3.34 eV in undoped ZnO cannot be found in 3 at % Ho doped ZnO sample and a small red shift to 3.06 eV was detected for the band attributed to $Zn_i \rightarrow$ VB electron transition. Moreover, a decrease of about 3.5 and 1.3 times in the peaks intensities can be observed for the 1 at % and 3 at % Ho doped ZnO, respectively, with respect to the undoped ZnO thin films. The emission intensities are determined by the radiative and nonradiative transitions, and the nonradiative transitions are generally induced by crystal imperfections, such as oxygen vacancies in ZnO thin films which could determine the reduction of the ZnO excitonic peak intensity. Usually, dopant incorporation in ZnO matrix could favor the defects formation. As can be seen in Figure 8 a, the intensity of the ZnO excitons emission increases with the Ho concentration. This direct observation allows us to conclude that the solubility of Ho ions in ZnO matrix is low and the excitonic emission is perturbed by other factors when the Ho concentration increases. On the other hand, the presence of defects such as oxygen vacancies, interstitial oxygen, interstitial zinc or zinc vacancies are usually observed in the visible region of the spectrum.[39] In our case, no visible emission can be visually detected in the PL spectrum of the undoped ZnO thermally treated at 500 °C (Figure 8 a)). This finding was already reported[36] and may suggest a high crystallographic quality of the ZnO films. The presence of $Ho^{3+}$ ions induces modifications in ZnO matrix and the stoichiometry between Zn and O atoms is disturbed, in agreement with the presence of some emission bands in the visible region (510 nm – 700 nm). In particular, three minor bands can be observed

in Figure 8 b: the first at 510 nm, the second at 564 nm and the third at 615 nm. The origins of the visible emissions are largely debated in the literature and different opinions exists. The green emission at 510 nm is usually attributed in the literature[37, 38] to the electron transition from the CB to interstitial oxygen ($O_i$). The band centered at 564 nm (2.2 eV) is described in the literature[40] as being determined by the electron transition process from the CB to a $V_O^{++}$ vacancy. These kinds of vacancies are effectives when a small difference between the depletion width and the grain size exists. In this case, most of $V_O^{+}$ are transformed into $V_O^{++}$ by trapping a hole from the grain surface. Therefore, this emission is strongly related to the surface defects and it was obviously detected, in our case, only in 1 at % and 3 at % Ho doped ZnO samples. The band centered at 615 nm (2.01 eV) was related to the electron transition from $Zn_i$ energy level to $O_i$.[38, 41] For the 5 at % Ho film, the ZnO lattice is strongly affected, the ZnO grain size becomes smaller (<10 nm, but still having a wurtzite structure, according to XRD and HRTEM), and have a different morphology than the rest of the samples (SEM). The strong and broad peak shifted at ~ 420 nm, which can be easily observed in Figures 8 a and 8 f, may originate from a different source of luminescence than the rest of the samples. I. Shalish *et al.*[42] explained that below a certain size, luminescence properties of the ZnO systems, which are in their case nanowires, should be *entirely* dominated by the properties of the surface. Most of the carriers excited throughout the volume can diffuse to the surface, and henceforth, *surface recombination prevails*. This is true as long as the pumping rate does not exceed the surface-recombination rate, as a high enough pumping rate may still produce band-to-band recombination (because only the surface states are capable of recombining a limited number of carriers at a given time).[42] In our case, a possible explanation is that the band-to-band recombination is strongly reduced, in relative proportion, as no ZnO excitons emission can be observed; also, the observed behavior may originate from a strong red shift of the exciton peak due to the presence of dominant defects such as interstitial zinc (~2.9 eV), zinc vacancies (3.03 eV) and interstitial oxygen (2.24 eV).

Unambiguously, the emission peak at ~ 662 nm (Figure 8b) could be attributed to the $Ho^{3+}$ transition ($^5F_5 \rightarrow {}^5I_8$) band, although its intensity is poor as compared to the ZnO excitonic emission. According to the previous literature,[16, 23] no emissions were observed so far for Ho doped ZnO bulk, single-crystal and epitaxial films using a UV light excitation source. However, Fabitha *et al*. observed $Ho^{3+}$ emissions in the range of 640-667 nm in their ZnO thin films.[30] It was explained as $^5F_5 \rightarrow {}^5I_8$ interband transition.

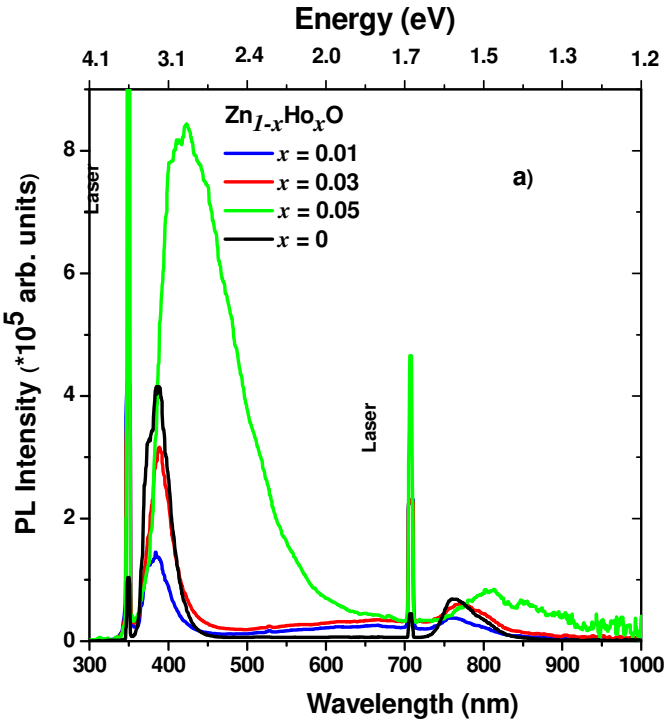
Energy (eV)
4.1
3.1
2.4
2.0
1.7
1.5
1.3
1.2
Zn1-xHoxO
x = 0.01
x = 0.03
x = 0.05
x = 0
a)
Laser
Laser
PL Intensity (*10^5 arb. units)
0
2
4
6
8
300
400
500
600
700
800
900
1000
Wavelength (nm)

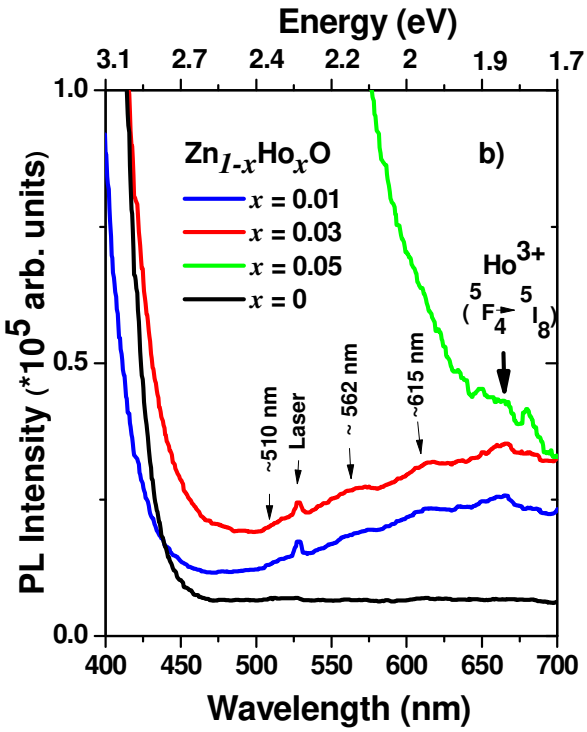
Energy (eV)
3.1
2.7
2.4
2.2
2
1.9
1.7
Zn1-xHoxO
x = 0.01
x = 0.03
x = 0.05
x = 0
b)
Ho3+
(5F4 → 5I8)
~510 nm
Laser
~ 562 nm
~615 nm
PL Intensity (*10^5 arb. units)
0.0
0.5
1.0
400
450
500
550
600
650
700
Wavelength (nm)

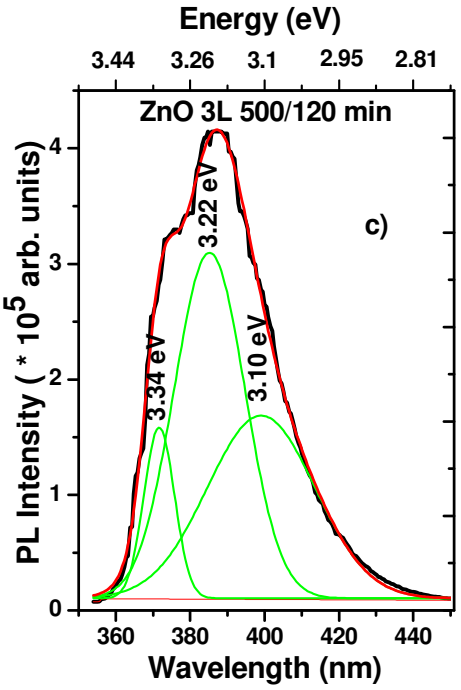
Energy (eV)
3.44 3.26 3.1 2.95 2.81
ZnO 3L 500/120 min
c)
3.34 eV
3.22 eV
3.10 eV
PL Intensity ( * 10^5 arb. units)
Wavelength (nm)

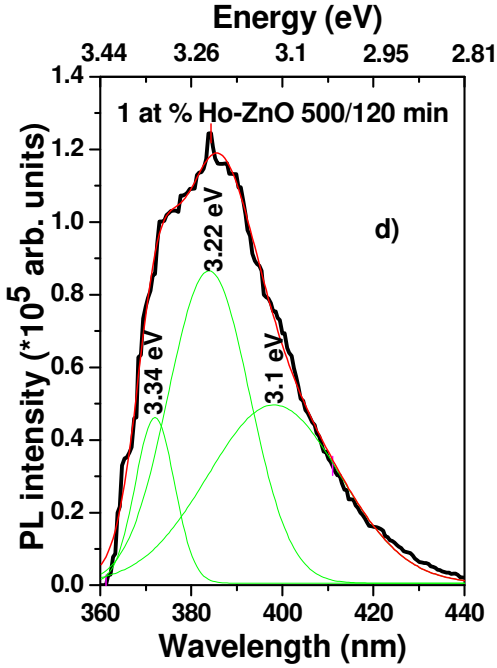
Energy (eV)
3.44 3.26 3.1 2.95 2.81
1 at % Ho-ZnO 500/120 min
d)
3.34 eV
3.22 eV
3.1 eV
PL intensity (*10^5 arb. units)
Wavelength (nm)

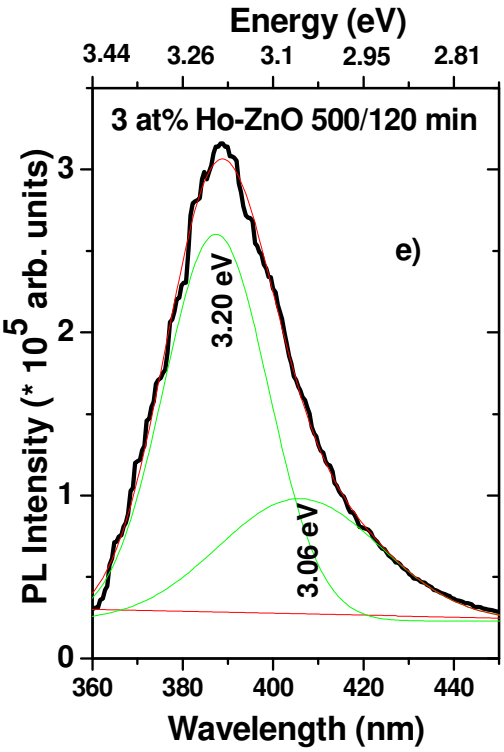
Energy (eV)
3.44 3.26 3.1 2.95 2.81
3 at% Ho-ZnO 500/120 min
e)
3.20 eV
3.06 eV
PL Intensity (* 10^5 arb. units)
Wavelength (nm)

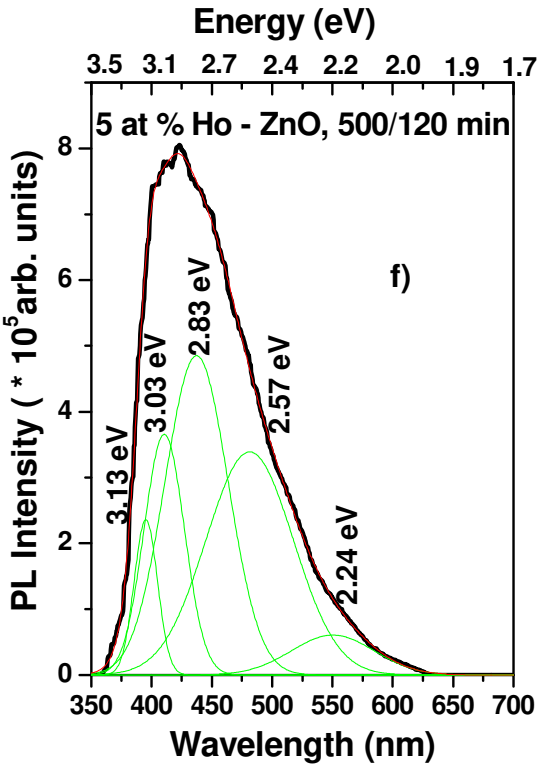
Energy (eV)
3.5 3.1 2.7 2.4 2.2 2.0 1.9 1.7
5 at % Ho - ZnO, 500/120 min
f)
3.13 eV
3.03 eV
2.83 eV
2.57 eV
2.24 eV
PL Intensity ( * 10^5arb. units)
Wavelength (nm)

**Figure 8.** (a) Room temperature PL spectra of $Zn_{1-x}Ho_xO$ ($x$ = 0, 0.01, 0.03, 0.05) in the range of 350-1000 nm. (b) Visible emissions of $Zn_{1-x}Ho_xO$ ($x$ = 0, 0.01, 0.03, 0.05). Gaussian deconvolution of the peaks corresponding to (c) undoped ZnO, (d) 1 at % Ho-ZnO, (e) 3 at % Ho-ZnO, (f) 5 at % Ho- ZnO.

It is generally admitted that the rare earths (RE) emission, using UV excitation, is possible only when *i)* an energy transfer occurs from the ZnO to the RE ions, forming a double Schottky barrier at the interface between the grains, which is possible when the $RE^{3+}$ ions are located at the surface of the ZnO grain[23] or *ii)* a direct excitation of the 4f levels of the $RE^{3+}$ is occurring; the last case is favorable when the $RE^{3+}$ have energy levels in the UV region, feature that $Ho^{3+}$ ions did not show before (for instance, some of the possible $Ho^{3+}$ transitions observed in ZnO are: 450 nm ($^5F_3 \rightarrow ^5I_8$), 545 nm ($^5F_4$, $^5S_2 \rightarrow ^5I_8$), 657 nm ($^5F_5 \rightarrow ^5I_8$) and 758 nm ($^5I_4 \rightarrow ^5I_8$)).[43] Thus, for considering an energy transfer from the ZnO matrix to the $Ho^{3+}$ ions, the incorporation of $Ho^{3+}$ ions inside the ZnO grains would have to take place. As mentioned before, the incorporation of RE ions in ZnO induces strong distortions in the ZnO lattice and is generally accompanied by other charge-compensating lattice defects or impurities nearby.[16]

It is thus very probable that small amounts of Ho ions could be directly incorporated in the ZnO matrix. The *c* lattice parameter, calculated from XRD, indicate no visible modification for 1 at % and some modifications for 3 and 5 at % Ho. However, for the first case, a small amount of $Ho^{3+}$ is divided into several ZnO nanograins, making their influence difficult to be detected by XRD. According to the previous literature[44], the band-to-band excitation induces only the luminescence of the ZnO self-activated centers and the photoluminescence observed would be only a consequence of the reabsorption process by the $RE^{3+}$ions of the light emitted by the ZnO itself. A deeper analysis of the PL spectra (Figure 8 b) shows that some activation centers (interstitial zinc, oxygen vacancies etc., as mentioned before) can be observed in 1 at % and 3 at % Ho doped ZnO samples, sustaining the hypothesis that some Ho ions were incorporated in ZnO matrix. This behavior is also sustained by N. Jiang *et al.*[45] who demonstrated by EELS that $Yb^{3+}$ ions can diffuse several ten of nanometers into the ZnO nanopowders. Thus, the poor luminescent emission observed at ~ 662 nm could be explained by the inefficient transfer from ZnO activated centers to $Ho^{3+}$ ions which are located in the vicinity of the ZnO surface. Indeed, in an already formed Schottky barrier, the $Ho^{3+}$ ions located at the surface of the ZnO grains may easily trap the electrons from the ZnO surface levels.

$$Ho^{3+} + e^-_{surf} \rightarrow Ho^{2+}$$

$$Ho^{2+} + h^+_{VB} \rightarrow {}^*Ho^{3+} (^5F_5) \rightarrow Ho^{3+}(^5I_8) + h\nu$$

The holes, formed in the VB of ZnO after the absorption of the light, migrate to the surface of the grains and recombine with the excess electrons trapped at the surface levels or they oxidize the $Ho^{2+}$ions into a luminescent $^{*}Ho^{3+}$ excited state. This mechanism was proposed by Bachir *et al.*[23] for explaining the ZnO-$Tm^{3+}$ luminescence and was also previously used for explaining the cathodoluminescence of $RE^{3+}$ doped $Y_2O_3$[46]. It could also be effective in the case of our Ho doped ZnO thin films since the standard reduction potential of $Ho^{3+}$ is -2.8 V.

As can be seen in Figure 8 b, the intensities of the peaks at 662 nm are about the same for different Ho concentration (1 to 5 at %). This can be explained only by considering that a certain number of Ho ions are incorporated in the ZnO surface, creating surface defects and thus, facilitating the energy transfer form ZnO matrix to Ho ions. After this number is exceeded, the excess of Ho ions tends to agglomerate on the surface of ZnO, more probably as $Ho_2O_3$, where they may form a core-shell like structure and do not show any luminescence. On this regard, the presence of Ho ions at the surface of the individual ZnO grains was confirmed by the analysis of some typical STEM-HAADF images (Figure 9) in which the difference in the atomic numbers of Ho and Zn ($Z_{Ho}$ = 67, $Z_{zn}$ = 30) allows to evidence, by analyzing the image contrast, the presence of a core-shell structure.

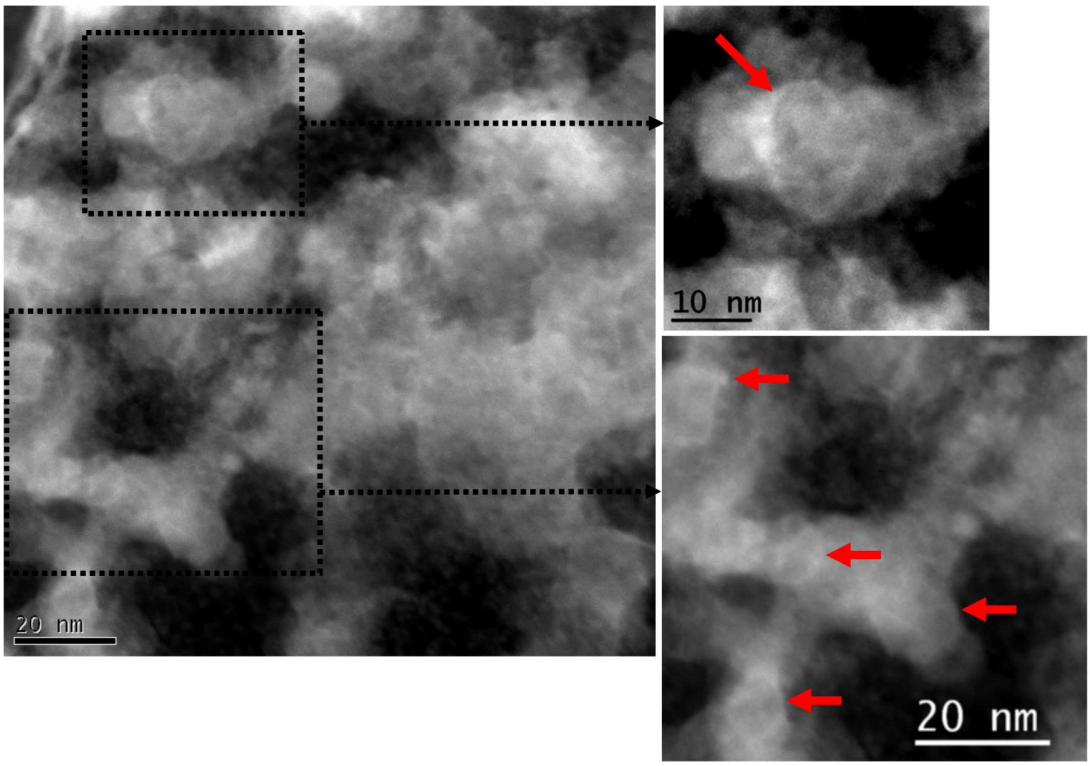

**Figure 9.** Typical STEM-HAADF images highlighting the presence of a core-shell like structure for the nanoparticles located in the Ho doped ZnO thin films.

## 4. Conclusion

Polycrystalline Ho doped ZnO thin films were prepared by the sol-gel method. The films are characterized by a wurtzite crystalline structure. Their morphology is homogeneous for 1 and 3 at % Ho doping amount and change in the 5 at% specimen. All the films show high transmission optical properties and the band gap energy decreases from 3.28 eV in undoped ZnO till 3.22 eV in $Zn_{0.95}Ho_{0.05}O$ films. The analysis of the photoluminescence spectra acquired at room temperatures evidences the presence of a red-light emission of $Ho^{3+}$(associated to the $^5F_5 \rightarrow ^5I_8$ transition at ~ 662 nm), under UV excitation. The presence of this emission line was correlated to the specific structure and the morphology of the films. Based on a multiselective structural analysis, using principally various TEM characterization tools, we were able to propose a structural mechanism that originates from the incorporation of Ho ions into the ZnO nanograins; once a doping limit exceeded, the Ho ions tend to agglomerate at the surface of ZnO grains leading to the formation of a core-shell like structure. The peculiar emission line observed at ~ 662 nm can be considered as a consequence of the energy transfer from the ZnO matrix, through structural defects (interstitial zinc, oxygen vacancies), to the incorporated Ho ions.

**Acknowledgements**:

The manuscript is dedicated to Dr. Virginia Danciu, researcher at UBB on the occasion of her 72th birthday.

**Conflicts of Interest**: The authors declare no conflict of interest. The funders had no role in the design of the study; in the collection, analyses, or interpretation of data; in the writing of the manuscript, or in the decision to publish the results.

## References


1. Pap, Z., et al., *TiO2/WO3/Au/MWCNT composite materials for photocatalytic hydrogen production: Advantages and draw-backs.* Physica Status Solidi (B) Basic Research, 2012. **249**(12): p. 2592-2595.
2. Pop, L.C., S. Sfaelou, and P. Lianos, *Cation adsorption by mesoporous titania photoanodes and its effect on the current-voltage characteristics of photoelectrochemical cells.* Electrochimica Acta, 2015. **156**: p. 223-227.
3. A. Janotti, C.G.V.d.W., *Fundamentals of zinc oxide as a semiconductor.* Rep. Prog. Phys., 2009. **72**: p. 126501(1-29).
4. M. Popa, R.A.M., M. Filip, M. Gabor, T. Petrisor Jr. L.Ciontea, T. Petrisor *Highly c-axis oriented ZnO thin films using 1-propanol as solvent in sol-gel synthesis.* Mater. Lett., 2013. **92**: p. 267-270.
5. Sarf, F., et al., *The role of rare-earth metal (Y, Ru and Cs)-doped ZnO thin films in NH3 gas sensing performances at room temperature.* Journal of Materials Science: Materials in Electronics, 2020. **31**(13): p. 10084-10095.
6. He, L., et al., *Investigation of 4f-Related Electronic Transitions of Rare-Earth Doped ZnO Luminescent Materials: Insights from First-Principles Calculations.* ChemPhysChem, 2020. **21**(1): p. 51-58.
7. Benosman, F., et al., *Investigated electronic structure and magnetic ordering of rare earth impurities (Eu, Gd) in ZnO.* International Journal of Modern Physics B, 2016. **30**(31).
8. Li, S., et al., *Structural and photoluminescence properties of Yb/Tm co-implanted ZnO crystals.* Physica B: Condensed Matter, 2017. **527**: p. 57-60.
9. Cerrato, E., et al., *Rare earth ions doped ZnO: Synthesis, characterization and preliminary photoactivity assessment.* Journal of Solid State Chemistry, 2018. **264**: p. 42-47.
10. Kalaiezhily, R.K., et al., *Tuning violet to green emission in luminomagnetic Dy,Er co-doped ZnO nanoparticles.* Ceramics International, 2018. **44**(16): p. 19560-19569.
11. Yang, L., et al., *The doping site analysis and control of Eu3+ in ZnO:Eu crystal lattice.* Journal of Luminescence, 2018. **204**: p. 189-194.
12. Goel, S., N. Sinha, and B. Kumar, *3D hierarchical Ho-doped ZnO micro-flowers assembled with nanosheets: A high temperature ferroelectric material.* Physica E: Low-Dimensional Systems and Nanostructures, 2019. **105**: p. 29-40.
13. S.J. Pearton, D.P.N., K. Ip, Y.W. Heo, T. Steiner, *Recent progress in processing and properties of ZnO.* Prog. Mater. Sci. , 2005. **50**: p. 293–340.
14. X. M. Teng, H.T.F., S. S. Pan, C. Ye, G. H. Li, *Influence of annealing on the structural and optical properties of ZnO:Tb thin films.* J. Appl. Phys. , 2006. **100**: p. 053507-1-5.
15. T. Ohtake, N.S., T. Sakata *Electrochemical luminescence of n-type ZnO semiconductor electrodes doped with rare earth metals under the anodic polarization* Appl. Surf. Sci., 2006. **253**: p. 1753-1757.
16. W. M. Jadwisienczak, H.J.L., A. Xu, B. Patel, *Visible Emission from ZnO doped with Rare-Earths Ions.* J. Electronic Mater. , 2002. **31**: p. 776-784.
17. L. Lu, T.P., K. Fana, K. Dai, *Effects of rare earth ion modifications on the photoelectrochemical properties of ZnO-based dye-sensitized solar cells* Renew. Energy 2011. **36**: p. 3386-3393.
18. J.C. Ronfard-Haret, V.W., J. Kossanyi *Triboluminescence of trivalent rare earth ions inserted in polycrystalline zinc oxide.* J. Lumin., 2000. **91**: p. 71-77.

19. X. Zeng, L.Z., *Synthesis and Photoluminescent Properties of Rare Earth Doped ZnO Hierarchical Microspheres.* J. Phys. Chem. C, 2008. **112**: p. 3503 - 3508.
20. M. Peres, S.P., M.R. Correia, M.J. Soares, A. Neves, M.C. Carmo, T. Monteiro, A.S. Pereira, M.A. Martins, T. Trindade, E. Alves, S.S. Nobre, R.A. S. Ferreira, *Optical studies of ZnO nanocrystals doped with Eu3+ ions.* Appl. Phys. A, 2007. **88**: p. 129-133.
21. Abou-Helal, M.O., *Rare earth ion doped semiconducting films by spray pyrolysis.* J. Non-Cryst. Solids, 1997. **218**: p. 139-145.
22. M. Godlewski, K.S., A. Suchocki and J.M. Langer, *Excitonic mechanism of luminescence excitation of rare-earths and transition metals in solids.* J. Lumin., 1991. **48 & 49**: p. 23-28.
23. S. Bachir, K.A., J. Kossanyi, P. Valat, J. C. Ronfard-Haret, *Photoluminescence of polycrystalline zinc oxide co-activated with trivalent rare earths ions and lithium. Insertion of rare-earth ions into zinc oxide.* J. Lumin., 1997. **75**: p. 35-49.
24. Röder, R., et al., *Transition Metal and Rare Earth Element Doped Zinc Oxide Nanowires for Optoelectronics.* physica status solidi (b), 2019. **256**(4): p. 1800604.
25. I. Soumahoro, A.D., S. Colis, M. Abd-Lefdil, N. Hassanain, A. Berrada, D. Muller, A. Slaoui, H. Rinnert, A. Dinia, *Structural, optical, and electrical properties of Yb-doped ZnO thin films prepared by spray pyrolysis method.* J. Appl. Phys., 2011. **109**: p. 033708 (1-5).
26. Ronfard-Haret, J.C., J. Kossanyi, and J.L. Pastol, *Electroluminescence of the Er3+ ion and electric conduction in polycrystalline ZnO:Mn,Bi,Er sintered pellets.* Journal of Physics and Chemistry of Solids, 2001. **62**(3): p. 565-578.
27. Park, Y.-K., et al., *Time-resolved spectroscopic study of energy transfer in ZnO:EuCl3 phosphors.* Journal of Luminescence, 1998. **78**(1): p. 87-90.
28. Wang, D., et al., *Defects-Mediated Energy Transfer in Red-Light-Emitting Eu-Doped ZnO Nanowire Arrays.* The Journal of Physical Chemistry C, 2011. **115**(46): p. 22729-22735.
29. J.C. Boyer, J.A.C., *Optical transitions and upconversion properties of Ho3+ doped ZnO-TeO2 glass.* J. Appl. Phys., 2003. **93**: p. 9460 - 9465.
30. Fabitha, K. and M.S. Ramachandra Rao, *Ho3+-doped ZnO nano phosphor for low-threshold sharp red light emission at elevated temperatures.* Journal of the Optical Society of America B: Optical Physics, 2017. **34**(12): p. 2485-2492.
31. Ermiş, I., et al., *Microstructure and Electrical Conductivity of ZnO Addition on the Properties of (Bi0.92Ho0.03Er0.05)2O3.* Journal of Electronic Materials, 2016. **45**(11): p. 5860-5866.
32. G. M. Rai, Y.X., I. G. Will, *Influence of Rare Earth Ho3+ Doping on Structural, Microstructural and Magnetic Properties of ZnO Bulk and Thin Film Systems.* Chin. J. Chem. Phys., 2011. **24**: p. 353 - 357.
33. Achehboune, M., et al., *Holmium (Ho)-coated ZnO nanorods: an investigation of optoelectronic properties.* Journal of Materials Science Materials in Electronics, 2020.
34. Kabongo, G.L., et al., *Photoluminescence Quenching and Enhanced Optical Conductivity of P3HT-Derived Ho(3+)-Doped ZnO Nanostructures.* Nanoscale research letters, 2016. **11**(1): p. 418.
35. Mereu, R.A., et al., *Synthesis and characterization of undoped, Al and/or Ho doped ZnO thin Films.* Ceramics International, 2013. **39**(5): p. 5535-5543.
36. J. Petersen, M.G., G. Schmerber, P. Gilliot, C. Ulhaq-Bouillet, J.-L. Rehspringer, S. Colis, C. Becker, A. Slaoui, A. Dinia *Correlation of structural properties with energy transfer of Eu-doped ZnO thin films prepared by sol-gel process and magnetron reactive sputtering.* J. Appl. Phys., 2010. **107**: p. 123522(1-6).

37. B. Cao, H.Z., *Temperature-dependent shifts of three emission bands for ZnO nanoneedle arrays.* Appl. Phys. Lett., 2006. **88**: p. 161101-161103
38. C. H. Ahn, Y.Y.K., D. C. Kim, S. K. Mohanta, H. K. Cho, *A comparative analysis of deep level emission in ZnO layers deposited by various methods.* J. Appl. Phys., 2009. **105**: p. 013502-5.
39. J. Petersen, M.G., O. Crégut, G. Schmerber, P. Gilliot, B. Hönerlage, C. Ulhaq-Bouillet, J. L. Rehspringer, C. Leuvrey, S. Colis, A. Slaoui, A. Dinia, *Optical properties of ZnO thin films prepared by sol-gel process.* Microelectron. J., 2009. **40**: p. 239 - 241.
40. J.D. Ye, S.L.G., F.Qin, S.M. Zhu, S.M. Liu, X. Zhou, W. Liu, L.Q. Hu, R. Zhang, Y. Shi, Y.D. Zheng, *Correlation between green luminescence and morphology evolution of ZnO films.* Appl. Phys. A, 2005. **81**: p. 759-762.
41. B. Cao, W.C., H. Zeng, *Temperature-dependent shifts of three emission bands for ZnO nanoneedle arrays.* Appl. Phys. Lett. , 2006. **88**: p. 161101-3
42. I. Shalish, V.N., *Size-dependent surface luminescence in ZnO nanowires.* Phys. Rev. B, 2004. **69** p. 245401-245404.
43. T. Ohtake, S.H., N. Sonoyama, T. Sakata, *Electrochemical luminescence of n-type ZnO semiconductor electrodes doped with rare earth metals under the anodic polarization.* Appl. Surf. Sci., 2006. **253**: p. 1753-1757.
44. J. Kossanyi, J.C.R.-H., P. Valat, J. Pouliquen, U. Mammel, D. Oelkrug, G. P. Kelly, F. Wilkinson, *Photoluminescence of semiconducting zinc oxide containing rare earth ions as impurities.* J. Lumin., 1990. **46**: p. 17-24.
45. N. Jiang, S.Y., J. Qiu, *Electron energy-loss spectroscopy study of Yb doped ZnO.* J. Appl. Phys., 2010. **108**: p. 083535-4.
46. Ozawa, L., *Cathodoluminescence: Theory and Applications*. 1990: Wiley.

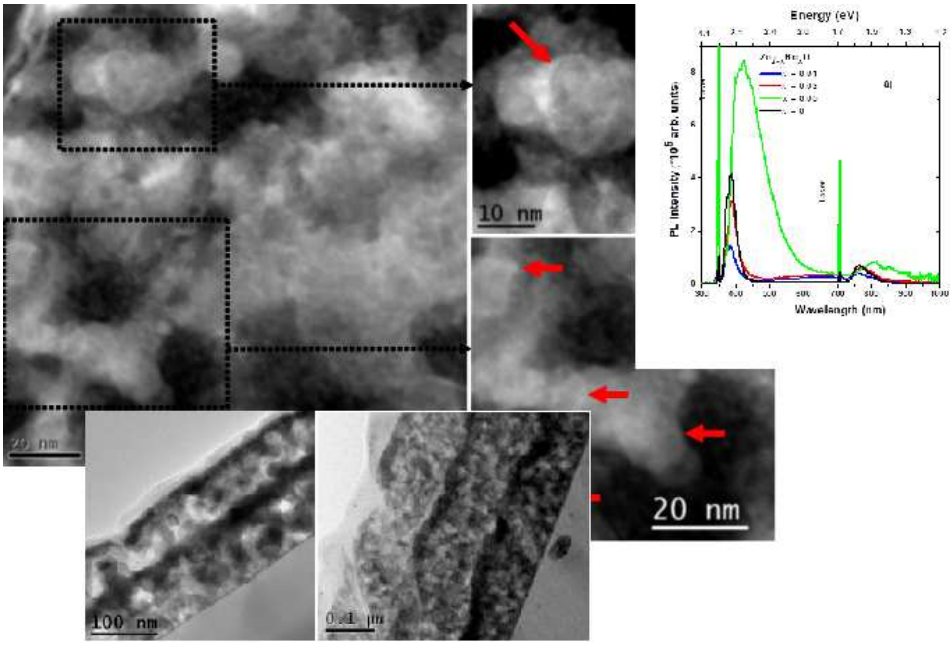
10 nm
20 nm
100 nm
0.1 μm
Energy (eV)
PL Intensity (10^5 arb. units)
Wavelength (nm)